

See discussions, stats, and author profiles for this publication at: <https://www.researchgate.net/publication/230311781>

Electron Density and Chemical Bonding: The Shape of Independent Atoms in Molecules

ARTICLE *in* BERICHTE DER BUNSENGESELLSCHAFT/PHYSICAL CHEMISTRY CHEMICAL PHYSICS · NOVEMBER 1992

DOI: 10.1002/bbpc.19920961106

CITATIONS

5

READS

8

4 AUTHORS, INCLUDING:



[Stephan Irle](#)

Nagoya University

203 PUBLICATIONS 3,254 CITATIONS

[SEE PROFILE](#)



[W H Eugen Schwarz](#)

Universität Siegen

199 PUBLICATIONS 3,834 CITATIONS

[SEE PROFILE](#)

Electron Density and Chemical Bonding: The Shape of Independent Atoms in Molecules

S. Irle, H. L. Lin, J. E. Niu, and W. H. E. Schwarz*)

Theoretische Chemie, Universität Siegen, PO Box 101240, D-5900 Siegen, Germany

Chemical Bond / Crystal Structure / Electron Densities / Molecular Structure

Electron density distributions $\rho(r)$ contain three types of features, which give rise to a new natural approach of analyzing ρ with respect to chemical bonding. These features are 1) the very large spherical atomic core densities, defining the geometric structure, 2) the small multipolar atomic valence densities, defining the orientation and population of partially filled p- and d-shells of the "independent atoms" in the molecule or crystal, and 3) the very small density deformations due to the interatomic interactions. The valence shell parameters and the Chemical Deformation Densities are determined theoretically and experimentally for molecules and crystals. The features are brought in relation to intramolecular and intramolecular interactions.

1. Introduction

It is rather common belief that the Electron Density Distribution $\rho(r)$ (EDD) in molecules and crystals characterizes the various kinds of chemical bonds [1]. For instance, transfer of electron density towards the midpoint between two atoms is believed to indicate covalent bonding, while charge transfer from one atom to another should attest ionic bonding. Unfortunately there exist quite a few contradictory examples (see e.g. [2, 3]).

To a good approximation, $\rho(r)$ is just the superposition of atomic densities ρ^a , the so-called promolecular or procrystal density $\rho^{pro}(r) = \sum_a \rho^a$. The atomic core densities are orders of magnitude higher than the atomic valence shell densities, which are still an order of magnitude bigger than the genuine atomic charge deformations caused by interatomic interactions. Thus the information contained in the EDD may be classified quite naturally into three categories.

The dominant core densities determine the positions \mathbf{R} and vibrational tensors \mathbf{U} of the atomic cores, which are routinely determined from X-ray or electron diffraction data. The geometric structure is the starting point for the understanding of all chemical properties.

Subtracting now the optimally positioned atoms from the molecule, the second prominent density features will become visible. While closed shell core densities of independent atoms are spherical, their degenerate open valence shell densities with nonzero angular momentum (p-, d- or f-shells) are not completely specified. For instance, the one-electron hole in the 2p-shell of a fluorine atom in its unperturbed ground state may be in the $2p_x$ - or $2p_y$ - or $2p_z$ -AO, in a coherent superposition of all three (i.e. in a 2p-AO of general orientation), or in an incoherent superposition. Traditionally, a spherically symmetric, incoherently mixed ensemble of all states from the atomic ground configuration is chosen as the atomic reference in ρ^{pro} . Accordingly, we will call

$$\Delta\rho = \rho - \sum_a \rho_{\text{opt. positioned}}^a \quad (1)$$

the Traditional Difference Density (TDD).

In Fig. 1 the TDDs of B_2H_4 , N_2 and F_2 are shown. Obviously the molecular density changes, with respect to optimally positioned but spherically averaged unperturbed atoms, do not correlate with the covalent bond strength, nor with the number of lone pairs. The dominant features in these TDD maps rather show that p-block atoms are not spherical but quadrupolar in these molecules. It is therefore tempting to adjust not only the atomic core positions, but also the directions and populations of the open valence shells of the unperturbed reference atoms to the molecular or crystal density. The corresponding difference density

$$\delta\rho = \rho - \sum_a \rho_{\text{opt. positioned}}^a \quad (2)$$

describes the changes of the one-electron density of the independent atoms which are brought about, when the atoms become fixed at their optimal positions with optimal valence shell orientations by the interatomic interactions (see Fig. 2). Therefore we will call this $\delta\rho$ the genuine Chemical Deformation Density (CDD). The present discussion is summarized in Table 1.

The aim of this paper is threefold. First, the idea of simultaneously determining the core position parameters and the valence shell orientation parameters will be mathematically formulated in section "2. Procedure". Second, the approach will be applied to quantum-chemical electron densities of molecules and to X-ray diffraction data of crystals in section "3. Results". The orientation and shape parameters of atoms with open p-shells are obtained in sections 3.1 & 3.2. The atomic shapes happen to correlate much better with the bonding situation than the TDDs used so far. The orientations of the atomic valence shells are significantly influenced by intermolecular interactions. Third, the new Chemical Deformation Density maps will be presented and discussed in sections 3.3 to 3.5.

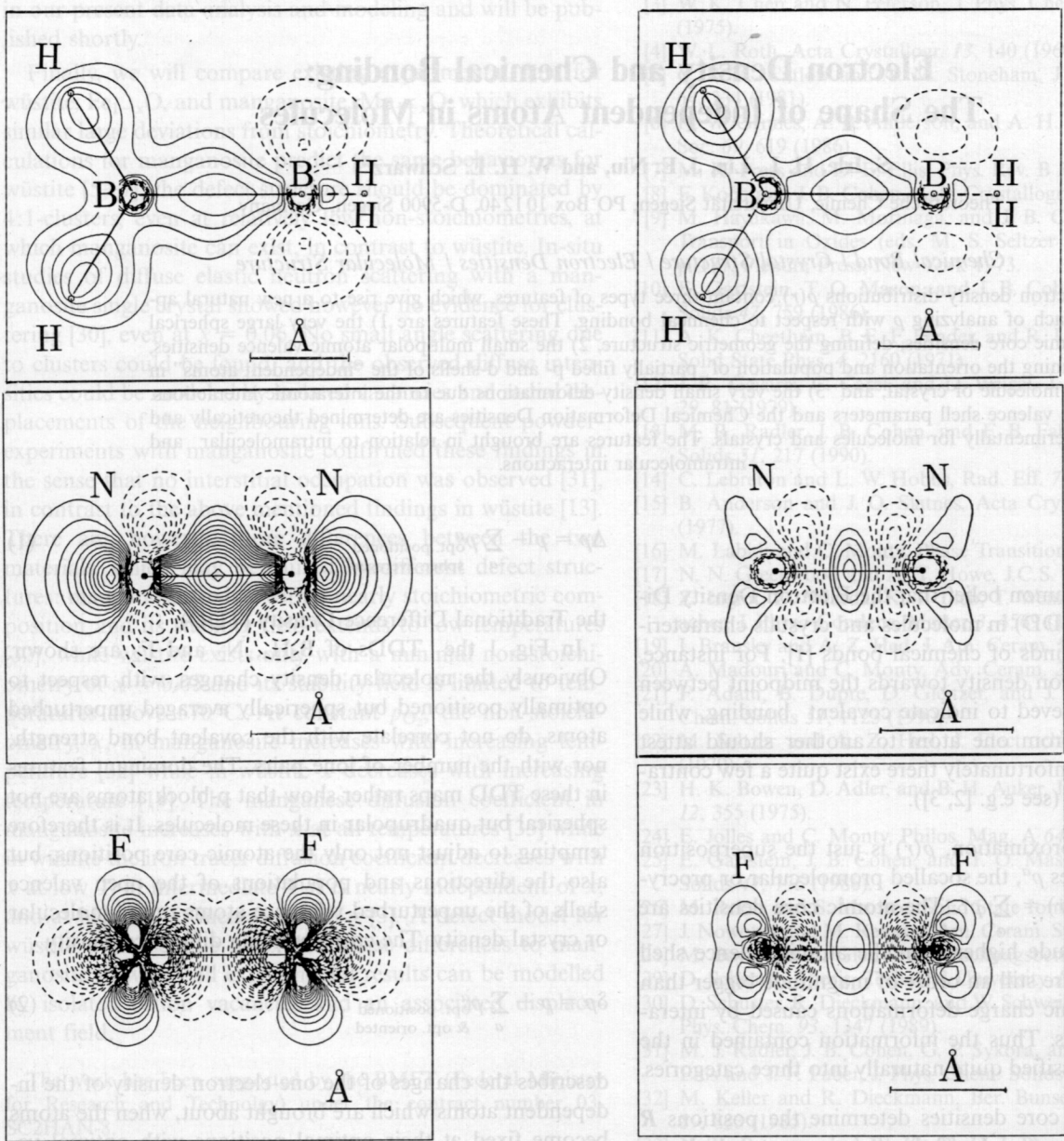


Fig. 1

Traditional Difference, TDD, $\Delta\rho = \rho - \sum \rho_{\text{spherical}}^a$ of B_2H_4 , N_2 and F_2 . Contour line values are $n \cdot 0.1 \text{ e}^{-\frac{r}{\text{\AA}}}$, $n = \pm 1, \pm 2, \pm 3, \dots$. Positive (—) and negative (----) difference density.

2. Procedure

In X-ray crystallography, \mathbf{R} and \mathcal{U} are usually determined with the help of the least mean squares method:

$$\left\langle |\rho - \sum_a \rho_{\text{spher}}^a (\mathbf{R}^a, \mathcal{U}^a)|^2 \right\rangle = \text{Min}. \quad (3)$$

Here, ρ is the electron density in momentum space, i.e. the squared structure factor, and $\langle \rangle$ means an integral or sum over the whole space, using an appropriate weight function. We extend this approach [4, 5] to determine \mathbf{R} , \mathcal{U} and \mathbf{P} , \mathcal{V} so that

Fig. 2

Chemical Deformation Density, CDD, $\delta\rho = \rho - \sum_a \rho_{\text{oriented}}^a$ of B_2H_4 , N_2 and F_2 . The optimized p-AO populations of the unperturbed atoms in the molecule are $\text{B } p_{\sigma}^{2.05} p_{\pi}^0$, $\text{N } p_{\sigma}^{1.54} p_{\pi}^{2.073}$, $\text{F } p_{\sigma}^{1.0} p_{\pi}^{2.20}$. Contour line values as in Fig. 1.

$$\left\langle |\rho - \sum_a \rho^a (\mathbf{R}^a, \mathcal{U}^a, \mathbf{P}^a, \mathcal{V}^a)|^2 \right\rangle = \text{Min}, \quad (4)$$

where \mathbf{P}^a denotes the population and \mathcal{V}^a the orientation of the open valence shell. In this manner, the populations $\mathbf{P}^a = (p_1, p_2, p_3)$ and the orientations \mathcal{V}^a of three orthogonal dumb-bell shaped Hartree-Fock ground state 2p-AOs of atoms B to F in different molecular and crystalline compounds have been determined. We now define a p-shell quadrupolar parameter

Table 1
Categories of information obtainable from electron density distributions

Density distribution	Main features	Physical meaning
EDD = total Electron Density Distribution, $\rho(r)$	maxima of the atomic core electron densities	chemical structure of the molecule: a) atomic coordinates, R (\Rightarrow bond lengths, bond angles) b) vibrational envelopes, U (\rightarrow valence force constants)
TDD = Traditional Difference Density $\Delta\rho = \rho - \sum_a \rho_{\text{spherical}}^a$	multipoles of the atomic open valence p- and d-shells	electronic structure of the atoms in the molecule: a) atomic orbital populations, P (\rightarrow bonding type) b) direction and shape of atomic orbitals, V
CDD = genuine Chemical Deformation Density $\delta\rho = \rho - \sum_a \rho_{\text{opt. orient}}^a$	lone pair dipoles, covalent bond charges	vestiges of covalent and ionic interactions, of atomic deformations and polarizations, of lone pair formations and nonbonded repulsions

$$q = p_1 - (p_2 + p_3)/2 \quad (5)$$

where indices 2 and 3 refer to the p-AOs with most similar populations. q determines the shape of the atomic 2p-shell density:

p-populations	q	atomic shape
$p_1 = p_2 = p_3$	0	spherical (ball)
$p_1 > p_2 \approx p_3$	>0	prolate (zigar)
$p_1 < p_2 \approx p_3$	<0	oblate (disk)
$p_1 \neq p_2 \neq p_3$	$\neq 0$	asymmetric ellipsoid

3. Results

3.1. Molecules

Second row molecules have been calculated with GAUSSIAN [6] at the Hartree-Fock level using double zeta polarized basis sets. From the corresponding electron densities, the populations and orientations of the 2p-AOs have been determined (compare [7]). They are represented with SCHAKAL [8] in Fig. 3 for three molecules. The length of a shaded rod is proportional to the population of the p-AO pointing in the respective direction.

The 2p-shell of the carbon atom in methan is spherically symmetric due to the high symmetry of the H-ligands. The C in homopolar compounds like C_2H_6 or H_3CBH_2 (Fig. 3a) is nearly spherical.

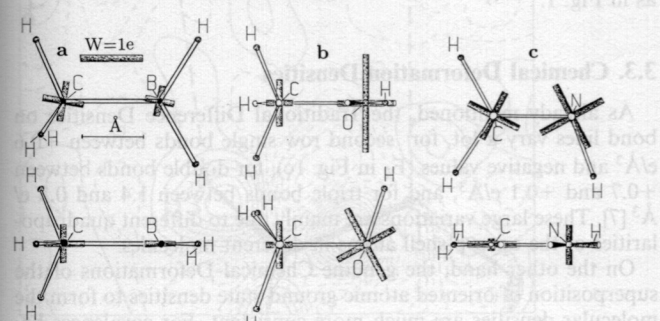


Fig. 3
Optimized directions and populations (~ length of the shaded rods) of the 2p-AOs of independent atoms in the three molecules a) H_3CBH_2 , b) H_3COH , c) H_2CNH ; front view and top view each.

Boron in a homopolar trigonal-planar surrounding is oblate with vanishing $p\pi$ population (Fig. 3a) and $q = -1/2$, as expected. If C is singly bonded to an electronegative, electron-rich atom E, its charge distribution becomes oblate, like a disk orthogonal to the C-E bond (H_3COH in Fig. 3b, $q(C) = -1/3$). The oxygen atom in H_3COH has two lone pairs; hence the two p-AOs in the corresponding directions have higher populations ($p_1 = 1.6$, $p_2 = 1.3$) than the p-AO tangential to the C-O-H grouping ($p_3 = 1.1$). Accordingly the O atom is an asymmetric zigar ($q = 0.4$) orthogonal to the bond plane.

The shape of multiply bonded atoms is unexpected at the first sight: a π -bond results in rather low population of the $p\pi$ -AOs, see e.g. H_2CNH in Fig. 3c. The carbon and nitrogen atom populations for the two pairs of $p\sigma$ -AOs in the molecular plane are 0.9 and 1.2, resp., whereas 0.2e and 0.6e, resp., in the vertical $p\pi$ -AOs are sufficient to simulate the molecular density. An additional π -bond reduces the σ -bond length so that the density along the bond line increases due to both better overlap and more efficient $p\sigma$ -interference. This molecular density is at best simulated by high $p\sigma$ -populations of the independent atoms in the promolecular reference density.

Summarizing, singly bonded atoms are approximately spherical, but slightly compressed (or expanded) in the direction towards an electron rich atom (or deficient atom, respectively). A good correlation of the carbon atom's q -parameters in H_3C-R molecules ($R = BH_2$, H, CH_3 , NH_2 , OH, F) with the electronegativity of the bonded element is shown in Fig. 4. Doubly bonded carbon atoms are oblate in the molecular plane ($q < 0$) and undergo similar compressions/expansions as the singly bonded C atoms upon variation of the electronegativity of the ligand. Finally, triply bonded carbon has two weakly populated $p\pi$ -AOs and one highly occupied $p\sigma$ -AO, its density forming a zigar ($q > 0$) parallel to the triple bond.

3.2. Molecular Crystals

As an example for the application to experimental X-ray diffraction data, we present results on crystals of the aromatic 1,2,3-triazine molecule $N_3C_3H_3$ in Table 2 (experimental data from MPI Mülheim [9]) and compare them with ab initio-SCF results of the free molecule.

Singly bonded nitrogen atoms are prolate in the lone pair (LP) direction with $p(LP) > p\sigma_1 \approx p\sigma_2$ and $q \approx +1/3$, whereas doubly bonded nitrogens are oblate in the lone pair–double bond–plane with $p(LP) \approx p$ (bond plane) $> p\pi$ and $q \approx -1/2$. The present case is intermediate with asymmetric nitrogen, $p(LP) > p\sigma$ (bond plane) $> p\pi$, indicating a reduced π -bond order between the nitrogens. The N-N distances in triazine are 1.326 Å, approximately the average between a N-N single bond (~1.43 Å) and a N=N double bond (~1.25 Å). This corresponds to a π -bond order of 0.5 without aromatic contraction and is in agreement with a rather small shared electron number of 0.29.

The carbon atoms in triazine, too, are significantly asymmetric (Table 2) with $p\sigma$ (radial) $> p\sigma$ (tangential) $> p\pi$ (with the exception of the C atoms in the 1,2,3-triazine molecule).

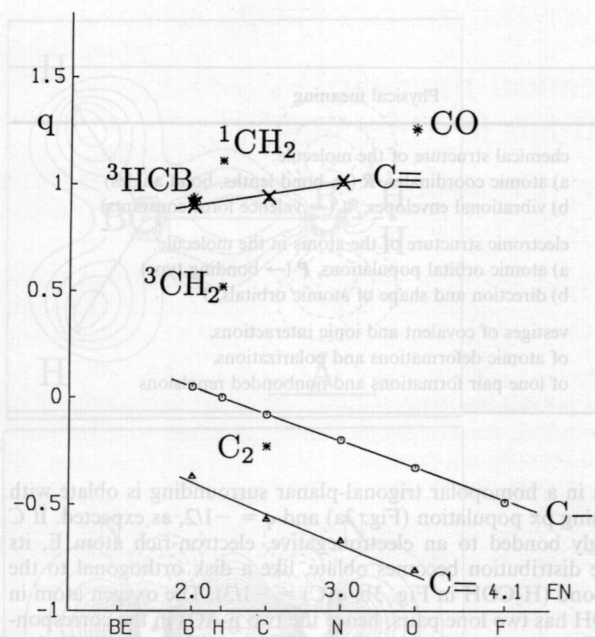


Fig. 4

Correlation of the quadrupolar parameter q (eq. 6) of independent carbon atoms in $H_nC \cdot R$ molecules with single ($C-$), double ($C=$), and triple ($C\equiv$) bonds versus the electronegativity EN of the atom bonded to C.

Table 2
AO-populations of 1,2,3-triazin crystals [9], SCF data for isolated molecules in parentheses

atom	radial $p\sigma^a)$	tangential $p\sigma$	$p\pi$
N_2	1.22 (1.37)	1.01 (0.95)	0.77 (0.68)
$N_1, N_3^b)$	1.50 ± 0.01 (1.34)	0.92 ± 0.02 (0.94)	(0.58 ± 0.01) (0.72)
$C_1, C_3^b)$	1.09 ± 0.06 (0.93)	0.64 ± 0.01 (0.79)	0.28 ± 0.07 (0.28)
C_2	1.03 (0.83)	0.60 (0.84)	0.36 (0.32)

a) Parallel to N-lone pair or to C-H bond.

b) Left-right average and variation.

tion of the theoretical populations for the central C_2), while singly bonded C are approximately spherical and doubly bonded C are symmetrically oblate. The $p\pi$ -occupation of carbon is much lower than that of nitrogen, indicating both the π bond character of the carbons and the polarization of the π -electrons towards nitrogen.

Summarizing, there is reasonable agreement between the AO-population parameters and the chemical bonding situation in the molecule. On the other hand, the experimental and theoretical data differ in some cases by more than the experimental statistical uncertainty (2σ of the population parameters $\approx 0.08e$). At present we do not know whether this discrepancy is due to experimental errors, due to theoretical errors, or due to intermolecular interaction effects.

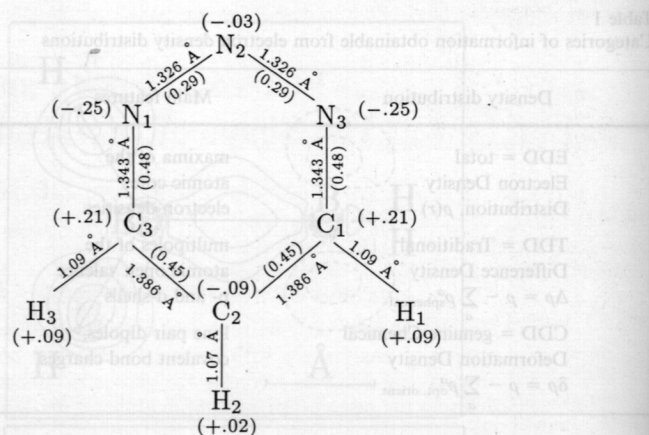


Diagramm: 1,2,3-triazine with experimental bond lengths in Å and theoretical SCF-Mulliken charges and shared electron numbers, in parentheses.

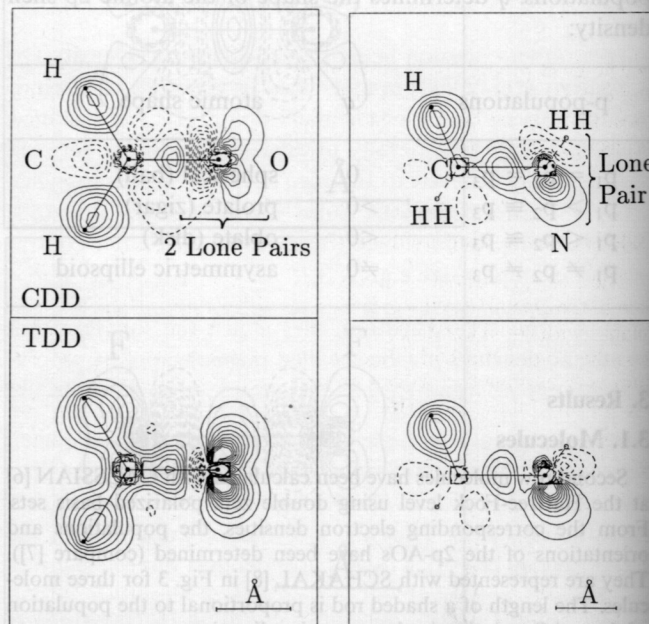


Fig. 5
Traditional Difference Density (TDD) and genuine Chemical Deformation Density (CDD) of H_3CNH_2 and H_2CO . Contour lines as in Fig. 1.

3.3. Chemical Deformation Densities

As already mentioned, the Traditional Difference Densities on bond lines vary a lot, for second row single bonds between $+0.6 e/\text{\AA}^3$ and negative values (F_2 in Fig. 1c), for double bonds between $+0.7$ and $+0.1 e/\text{\AA}^3$, and for triple bonds between 1.4 and $0.3 e/\text{\AA}^3$ [7]. These large variations are mainly due to different quadrupolarities of the open p-shell atoms in different molecules.

On the other hand, the genuine Chemical Deformations of the superposition of oriented atomic ground state densities to form the molecular densities are much more consistent. For covalences between the 2p-elements the CDD bond maxima are typically of the order of 0.3 to $0.5 e/\text{\AA}^3$, but may appear smaller if overlaid by lone pair – charge shift – dipoles. Remarkably, the CDD is also rather small for some of the multiply bonded molecules, for instance C_2H_2 [7]. The CDD is also small for polar and ionic molecules.

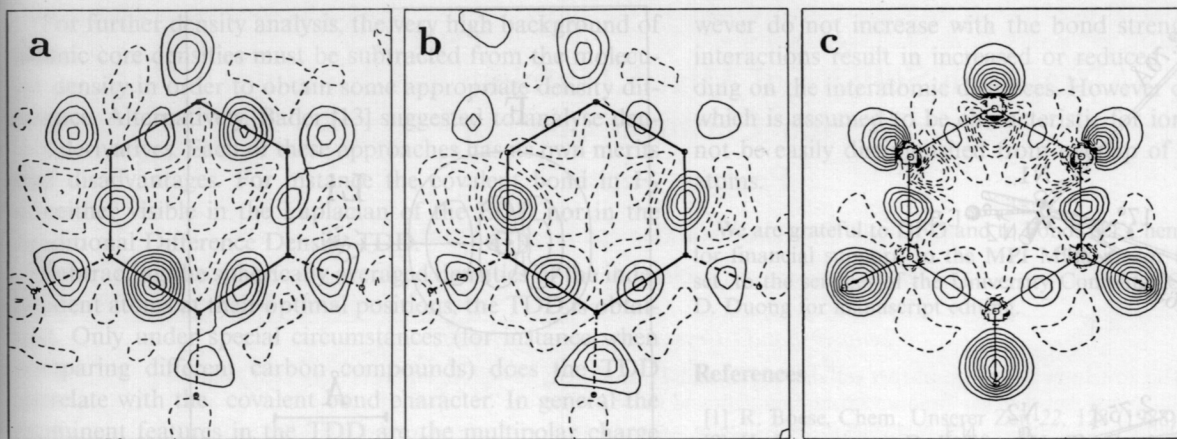


Fig. 6
DD maps of 1,2,3-triazine: experimental TDD (a) and CDD (b) of the crystal; ab initio-SCF CDD (c) of the free molecule. Contour lines values as in Fig. 1.

The most prominent features in the CDDs of free molecules are the dipolar features characteristic for lone pairs. In many TDDs these features are buried under the atomic valence shell quadrupoles as in F_2 (Figs. 1c, 2c) or in H_3CNH_2 and H_2CO (Fig. 5).

3.4. Intermolecular Interactions

The free 1,2,3-triazine molecule has C_{2v} symmetry, which is broken in the crystal. Yet the ring remains highly symmetric, i.e. nearly planar with equal bond lengths on the left and right side. Nevertheless the Traditional Difference Density of crystalline triazine becomes very asymmetric, as can be seen from Fig. 5a and Tab. 3. As we already know, the TDDs on the bonds do not correlate with

Table 3
TDD and CDD maxima of crystalline 1,2,3-triazine in $e/\text{\AA}^3$

	TDD	CDD	CDD (molecules, SCF)
N_2 lone pair	0.39	0.36	0.80
N_1-N_2/N_2-N_3 bond	0.28/0.53	0.11/0.25	0.18
N_1/N_3 lone pair	0.44/0.35	0.24/0.19	0.77
N_1-C_3/N_3-C_1 bond	0.35/0.28	0.45/0.45	0.45
C_2-C_3/C_1-C_2 bond	0.74/0.46	0.44/0.34	0.28
C_3-H_3/C_1-H_1 bond	0.37/0.37	0.32/0.26	0.80
C_2H_2 bond	0.29	0.38	0.90

the bond strengths. Even the CDDs will not do so, but vary much less, see Fig. 5b and Table 3. (The large deviation of the theoretical molecular CDD from the experimental crystal CDD in the CH bonds are probably due to typical X-ray crystallographic problems with hydrogen. In the lone pair areas also solid state effects may contribute).

The intermolecular interactions evidently strongly affect the electron density, but only weakly affect the intramolecular bonding. In fact, the population-parameters of the left and right atoms N_1 , C_3 and N_3 , C_1 are equal within ± 0.01 to ± 0.07 , whereas the statistical uncertainties are $2\sigma = \pm 0.08$. The intermolecular interactions rotate the atomic valence shell quadrupoles by up to 20° without changing the quadrupole values and the chemical bond strengths appreciably.

Triazine forms a layer crystal with short CH–N contacts within a layer ($H-N$ distances of 2.43, 2.55 and 2.65 Å, the van der Waals radii sum being 2.6 Å) and long $CH \cdots N$ interactions between the layers (2.7 to 3.1 Å). In Fig. 7 we show a corresponding cut through the CDD. The electrostatic interactions between the H^{+8} and N^{-8} atoms of different layers result in polarizations of the N -lone pair densities and CH-bond densities towards each other so that there is hardly any negative CDD on the long $N \cdots H$ lines. At the shorter N–H contacts within the layers, the atomic van der Waals spheres begin to overlap; the Pauli exclusion principle favors more negative CDD values. Accordingly the molecules in the crystal are arranged in such a manner that the nitrogen lone pairs avoid the nearest contacts with the C–H bonds (Fig. 8); and the nitrogen p-AOs are somewhat rotated off their symmetry adapted orientations in the free molecules, what contribute to the TDD asymmetry in Fig. 5a.

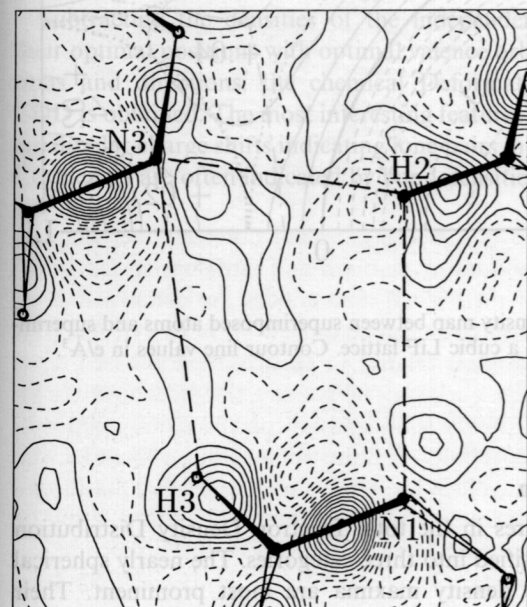


Fig. 7
Cut of the CDD in triazine crystal through two molecules of an upper layer (N_3-H_2 contact, 2.43 Å) and one molecule of the lower layer (N_3-H_3 distance 3.10 Å, H_2-N_1 distance 2.92 Å). Contour lines are $\pm n \cdot 0.05 e/\text{\AA}^3$.

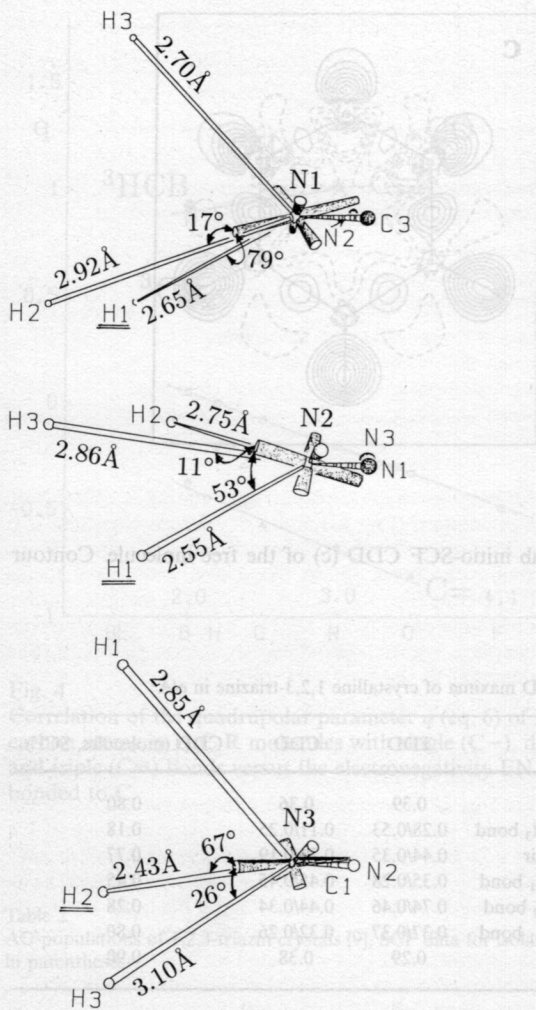


Fig. 8
The three nitrogen atoms of triazine, each surrounded by one H from the same layer and two ones from the next layers. The p-AO directions and populations on the N atoms are represented by shaded rods. Note the small angle between the “lone-pair p-AO” with highest population (longest rod) and the most distant H atom.

3.5. Ionic Deformation Densities

The CDD map of LiF is shown in Fig. 9. The F atom is nearly spherical ($p_{\sigma} = 1.7$, $p_{\pi} 1.65$) as to be expected for a typically ionic molecule of closed shell ions. There is a weak diffuse density decrease around the Li atom of less than $0.1 \text{ e}/\text{\AA}^3$ and a polarized weak density increase on the F atom of up to $0.3 \text{ e}/\text{\AA}^3$. The most accurate experimental electron Difference Density determination of Li_2BeF_4 crystals [10] obtained with the help of the most accurate atomic and ionic form factors [11] yielded even smaller charge accumulations on the F atoms in the solid ($\sim 0.1 \text{ e}$). These results represent the most sophisticated verification of the fact [12] that there is very little difference between a) the overlap of electronegative atoms (F) with the diffuse valence orbitals of the adjacent, densely packed electropositive atoms (Li) on one hand; and b) charge transfer between nearly nonoverlapping negative and positive ions (F^- , Li^+) on the other hand. The difference between a neutral atomic and a charged ionic [LiF]-procrystal is indeed extremely small (see Fig. 10).

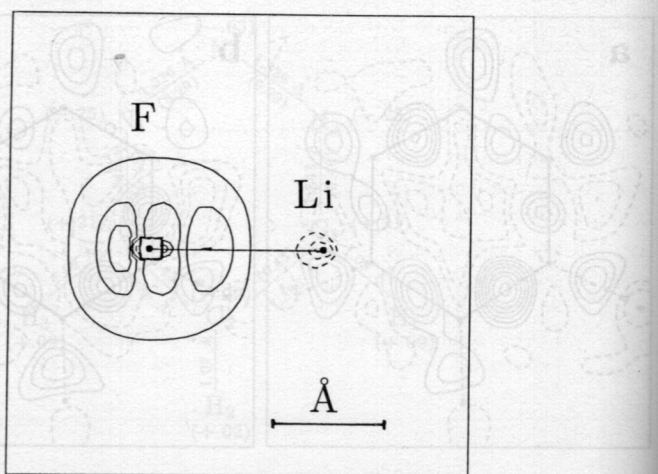


Diagramm 1,2,4-triazine with experimental bond lengths in Å and shared electron numbers. CDD map of LiF, contour line values as in Fig. 1.

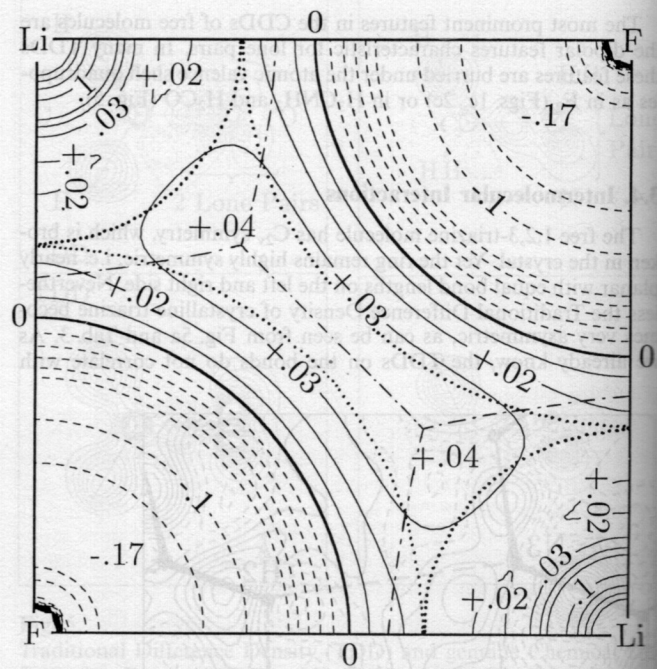


Fig. 10
Difference density map between superimposed atoms and superimposed ions in a cubic LiF lattice. Contour line values in $\text{e}/\text{\AA}^3$.

4. Discussion

The features in the total Electron Density Distribution may be classified into three categories. The nearly spherical atomic core density maxima are most prominent. Their analysis yields those atomic positions which are optimal for the interactions in the molecule or crystal. That is, the most important chemical information from electron density distributions about interatomic interactions in matter (chemical bonds) is the geometrical structure.

For further density analysis, the very high background of atomic core densities must be subtracted from the molecular density in order to obtain some appropriate density difference. Alternatively, Bader [13] suggested to analyse density derivatives. Each of these approaches has its own merits and disadvantages. For instance the covalent bond in F_2 is neither visible in the Laplacian of the EDD nor in the Traditional Difference Density TDD.

Subtracting the spherically averaged densities of the independent atoms at their optimal positions, the TDD is obtained. Only under special circumstances (for instance when comparing different carbon compounds) does the TDD correlate with the covalent bond character. In general the prominent features in the TDD are the multipolar charge distributions in the atomic open degenerate valence shells. Their analysis yields those populations, orientations, and shapes of the undeformed valence shells, which are optimal for the interatomic interactions. According to zero order perturbation theory, one has to select an appropriate state from the degenerate or near-degenerate ground-state manifold as the unperturbed zeroth order reference state. So an additional piece of information on bonding is the electronic structure of the atoms in the molecule, which correlates with bond order and polarity of the covalent bond. $p\pi$ bonding AOs are weakly populated and $p\sigma$ AOs in the direction of lone pairs and short multiple bonds are highly populated. The directions of the valence AOs are influenced by intermolecular interactions, thereby modifying the TDD without large influence on intramolecular binding. As has recently been shown [14], the classical electrostatic interaction energy of unperturbed, optimally positioned and oriented atoms forms an approximate estimate of twice the quantum mechanical bond energy.

Subtracting the densities of the independent atoms at their optimal positions with optimal valence orbital populations and directions, the chemical Deformation Density CDD is obtained. The most interesting features in the CDD are dipolar charge shifts indicating lone pairs in s-p-hybrids. Covalences are often indicated by bond densities, which ho-

wever do not increase with the bond strengths. Hydrogen interactions result in increased or reduced CDDs, depending on the interatomic distances. However charge transfer, which is assumed to be characteristic for ionic bonds, cannot be easily distinguished from overlap of diffuse neutral atoms.

We are grateful to DFG and to Fonds der Chemischen Industrie for financial support, to the MPI Mülheim for the triazine data set, to the services of the University Computer Center and to H. D. Duong for manuscript editing.

References

- [1] R. Boese, *Chem. Unserer Zeit* 22, 128 (1988).
- [2] H. Irngartinger, D. Kallfass, H. Prinzbach, and O. Klingler, *Chem. Ber.* 122, 175 (1989).
- [3] P. Seiler and J. D. Dunitz, *Helv. Chim. Acta* 69, 1107 (1986).
- [4] K. Ruedenberg and W. H. E. Schwarz, *J. Chem. Phys.* 92, 4956 (1990); L. L. Miller, R. A. Jacobson, K. Ruedenberg, W. H. E. Schwarz, and J. E. Niu, to be published.
- [5] W. H. E. Schwarz, K. Ruedenberg, and L. Mensching, *J. Am. Chem. Soc.* 111, 6926 (1989).
- [6] M. J. Frisch et al., *GAUSSIAN* 90, Gaussian Inc., Carnegie-Mellon University, Pittsburgh PA 1990.
- [7] W. H. E. Schwarz, H. L. Lin, S. Irle, and J. E. Niu, *J. Mol. Struct. (Teochem)* 255, 435 (1992).
- [8] E. Keller, *SCHAKAL*, Kristallographisches Institut, Universität Freiburg 1990.
- [9] A. Angermund, K. H. Claus, R. Goddard, and C. Krüger, *Angew. Chem.* 97, 241 (1985).
- [10] P. Seiler, in *Sagamore X Conference Proceedings*, p. 118, eds., M. Springborg, A. Saenz, and W. Weyrich, Universität Konstanz 1991, see also [3].
- [11] B. Hess, H. L. Lin, J. E. Niu, and W. H. E. Schwarz, *Z. Naturforsch. A*, in press 1992.
- [12] J. C. Slater, *Quantum Theory of Molecules and Solids*, Vol. 2, sec. 4-4. McGraw-Hill, New York 1965.
- [13] R. F. W. Bader, *Atoms in Molecules*, Clarendon, Oxford 1990.
- [14] S. G. Wang, W. H. E. Schwarz and H. L. Lin, *Chem. Phys. Lett.* 180, 509 (1991).

Presented at the 91st Annual Meeting of E 8065
the Deutsche Bunsen-Gesellschaft für
Physikalische Chemie „Festkörper: Ther-
modynamik, Struktur und Bindung“ in
Vienna, from May 28th to May 30th, 1992

Fig. 5
A Ta-Nb-S ternary diagram showing the phase diagram of the system. The observed phases include the solid solution of Ta_2S and Ta_3S and the liquid solution of Ta_2S . The phases ordinate Nb_2S and Ta_2Nb are not obtained.

The system consists of four main layers separated by pairs of sulfur layers. The first layer is isostructural with Ta_2S . The stoichiometries of these new ternaries as determined by refinement of single crystal data are given in Table 3.

What is remarkable is that the number of the tendency for higher coordination decreases with decreased sulfur coordination and the increasing metal-metal interaction (which is reflected in the decreasing third-order [17], $D_{30} = D(1) - 0.3 \log n$, Fig. 10). This correlation indicates that Ta_2 , presumably because of the greater radial extent of the 5d orbitals, segregates preferentially in situ into the two phases, leaving more room for increased metal-metal (M-M) bonding.